Image Thresholding Using
Micro Opposition-Based Differential Evolution (Micro-ODE)

Shahryar Rahnamayan[1], Hamid Reza Tizhoosh[2]

***Abstract*— Image thresholding is a challenging task in image processing field. Many efforts have already been made to propose universal, robust methods to handle a wide range of images. Previously by the same authors, an optimization-based thresholding approach was introduced. According to the proposed approach, Differential Evolution (DE) algorithm, minimizes dissimilarity between the input grey-level image and the bi-level (thresholded) image. In the current paper, micro Opposition-Based Differential Evolution (micro-ODE), DE with very small population size and opposition-based population initialization, has been proposed. Then, it is compared with a well-known thresholding method, Kittler algorithm and also with its non-opposition-based version (micro-DE). In overall, the proposed approach outperforms Kittler method over 16 challenging test images. Furthermore, the results confirm that the micro-ODE is faster than micro-DE because of embedding the opposition-based population initialization.**

I. Introduction

In many image processing applications, the crucial role of the image thresholding can be observed (e.g., medical image processing [1], [2]). Numerous thresholding techniques have already been proposed [3]–[6]. However, almost all of them are application- or domain-oriented solutions, suffering from lack of universality. Therefore, this research field is still open to investigation and introduction of new robust and universal techniques.

In the previously proposed thresholding technique by the authors [7], a new thresholding technique was proposed which generates corresponding binary image by minimizing the dissimilarity between the input and the output images. Hence, the grey-level input image itself is directly used to measure the quality of the thresholded image; thus, this method can be introduced as a candidate for universal thresholding. Differential Evolution (DE) is utilized as an optimizer in the mentioned minimization exercise. By this way, the thresholding task was changed to an optimization problem. In the current paper, in order to reduce computation time, DE with a very small population size ($N_p = 5$), called micro-DE, has been employed. A small population size results a shorter computation time which is a crucial factor for the image processing tasks to make them suitable for online applications (e.g., robotics or production line control).

After comprehensive evaluation of more than 40 image thresholding techniques, Sezgin and Sankur [3] concluded that the Kittler [8] is the best overall performing method. For this reason, and like many other thresholding works [5], the proposed method is compared with the Kittler. In the final part of this paper, as a case study, the micro-DE and micro-ODE (micro-DE equipped with opposition-based initialization [9], [10]) are compared in terms of convergence speed and robustness.

Organization of this paper is as follows: A short review of Differential Evolution is given in section II. The proposed image thresholding approach is presented in section III. Experimental investigation is provided in section IV. The micro-DE and micro-ODE are compared in section V. Finally, the paper is summarized and concluded in section VI.

II. A Short Review of Differential Evolution

Differential Evolution (DE) is a population-based and directed search method [11], [12]. Like other evolutionary algorithms, it starts with an initial population vector, which is randomly generated when no preliminary knowledge about the solution space is available.

Let us assume that $X_{i,G}(i = 1, 2, ..., N_p)$ are solution vectors in generation G (N_p =population size). Successive populations are generated by adding the weighted difference of two randomly selected vectors to a third randomly selected vector.

For classical DE ($DE/rand/1/bin$), the mutation, crossover, and selection operators are straightforwardly defined as follows:

Mutation - For each vector $X_{i,G}$ in generation G a mutant vector $V_{i,G}$ is defined by

$$V_{i,G} = X_{a,G} + F(X_{b,G} - X_{c,G}), \qquad (1)$$

where $i = \{1, 2, ..., N_p\}$ and a, b, and c are mutually different random integer indices selected from $\{1, 2, ..., N_p\}$. Further, i, a, b, and c are different so that $N_p \geq 4$ is required. $F \in [0, 2]$ is a real constant which determines the amplification of the added differential variation of $(X_{b,G} - X_{c,G})$. Larger

Postdoctoral Fellow, Department of Mechatronic System Engineering, Simon Fraser University, Vancouver, Canada, shahryar@sfu.ca
[2] Department of Systems Design Engineering, University of Waterloo, Waterloo, Canada, tizhoosh@uwaterloo.ca

978-1-4244-1823-7/08/$25.00

values for F result in higher diversity in the generated population and lower values cause faster convergence.

Crossover - DE utilizes the crossover operation to generate new solutions by shuffling competing vectors and also to increase the diversity of the population. For the classical version of the DE ($DE/rand/1/bin$), the binary crossover (shown by 'bin' in the notation) is utilized. It defines the following trial vector:

$$U_{i,G} = (U_{1i,G}, U_{2i,G}, ..., U_{Di,G}), \tag{2}$$

where $j = 1, 2, ..., D$ ($D =$ problem dimension) and

$$U_{ji,G} = \begin{cases} V_{ji,G} & \text{if } rand_j(0,1) \leq C_r \vee j = k, \\ X_{ji,G} & \text{otherwise.} \end{cases} \tag{3}$$

$C_r \in (0, 1)$ is the predefined crossover rate constant, and $rand_j(0, 1)$ is the j^{th} evaluation of a uniform random number generator. $k \in \{1, 2, ..., D\}$ is a random parameter index, chosen once for each i to make sure that at least one parameter is always selected from the mutated vector, $V_{ji,G}$. Most popular values for C_r are in the range of $(0.4, 1)$ [13].

Selection - The approach that must decide which vector ($U_{i,G}$ or $X_{i,G}$) should be a member of next (new) generation, $G + 1$. For a maximization problem, the vector with the higher fitness value is chosen. There are other variants based on different mutation and crossover strategies [14].

III. Proposed Image Thresholding Approach

When we are comparing the input grey-level image and corresponding thresholded version we perceptually map darker pixels in the input image to the black pixels in the thresholded image and lighter ones to the white pixels. With this method, we subjectively measure the quality of the thresholding. The same procedure happens even for a person who knows nothing about image processing concepts. We will have a high quality thresholded image when the mentioned similarity is high, or in other words, the dissimilarity is low. So, the thresholding task can be understood as an optimization problem. Before describing the new approach, the objective function for this optimization exercise should be defined.

Objective function - For an $M \times N$ input grey-level image I (normalized in $[0, 1]$), and the corresponding thresholded image $B(T) \in \{0, 1\}$ (T: threshold value), the objective function $f(T)$ is defined as follows [7]:

$$f(T) = \sum_{i=1}^{M} \sum_{j=1}^{N} |I_{ij} - B(T)_{ij}|. \tag{4}$$

Minimization of this objective function means minimizing the dissimilarity between the input image and the thresholded image (see Figure 1).

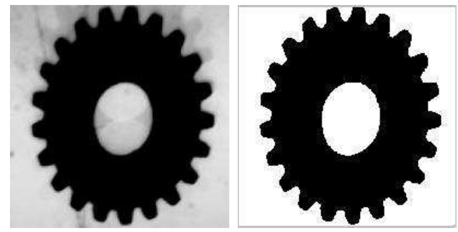

Fig. 1. A sample image to show that darker and lighter pixels in input grey-level image are matchable with black and white pixels in the thresholded image. In order to maximize the matching level, the dissimilarity between these two images, $f(T)$, should be minimized.

In order to solve this one-dimensional minimization problem, the DE with very small population size ($N_p = 5$), micro-DE, is utilized. The pseudo-code representation of the proposed thresholding approach is shown in Algorithm 1 [7].

Algorithm 1 Proposed Thresholding Approach (micro-DE version)

1: Random population initialization, P_0
2: Calculate objective value (dissimilarity measure) for each individual in the population
{DE's evolution steps}
3: **while** (satisfying termination criteria) **do**
4: Mutation
5: Crossover
6: Selection
7: **end while**
8: Thresholding input image with the found optimal value of thresholding level, T_{op}

IV. Experimental Verifications

In order to investigate the performance of the new approach, 16 hard-to-threshold images were selected; all images are frequently used in the image processing literature [3], [5].

The following micro-DE control parameters are set for all conducted experiments with no attempt to achieve their optimal values.

- Population size, $N_p = 5$
- Differential amplification factor, $F = 0.9$
- Crossover probability constant, $C_r = 0.9$

- Strategy: DE/rand/1/bin
- Maximum function calls, NFC_{MAX}=200 (300 for image no. 9)

Threshold results of applying the proposed approach are presented in Table I. As shown, also corresponding ground-truth image (created manually) and the result of the Kittler method are given for comparison. By visual evaluation, the new approach, at least over ten of the images (image no. 1,3,4,6,7,8,11,13,15,16) shows better results than Kittler.

For all images, plot of objective function $f(T)$ versus thresholding value T is presented in Figures 2 and 3. Furthermore, the result for the different thresholding values is given on each curve. Asymmetric shapes, flat surfaces, and also steep edges in the plotted graphs show that the objective function can be challenging although it is a one-dimensional problem.

A wide range of image quality measures have been proposed by image processing researchers [15]–[17]. In this section, results of Kittler and the proposed approach are compared by reference-based objective assessment. Reference or ground-truth images have been manually prepared to serve as gold/ideal thresholded image for each test image. To compare two binary images, Misclassification Error (ME) [3], [18] can be a reasonable and straightforward measure to use. It calculates the percentage of foreground pixels which have been assigned wrongly to background and vice versa:

$$ME = \frac{|B_O \cap F_T| + |F_O \cap B_T|}{|B_O| + |F_O|}, \tag{5}$$

where B_O, F_O, B_T, and F_T are the background and foreground pixels of the ground-truth image and the background and foreground pixels of the test image, respectively (see figure 4). $|\cdot|$ denotes the cardinality of the set.

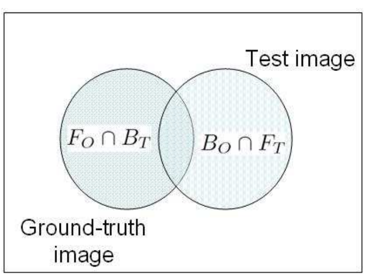

Fig. 4. Illustration of $B_O \cap F_T$ and $F_O \cap B_T$.

By utilizing this error measure, the similarity index η can be defined as follows:

$$\eta = (1 - ME) \times 100\%. \tag{6}$$

Table II summarizes the results of objective assessment for 16 test images. Results of the Kittler and new method are compared with the gold image. The best result, in each case has been indicated in boldface. According to the mentioned similarity index, the Kittler shows better results for 5 cases; micro-DE performs better for 10 cases; and for one case the results is almost the same (results with difference less than 1% are considered the same).

TABLE II
RESULTS OF OBJECTIVE ASSESSMENT FOR 16 TEST IMAGES. THE BEST RESULT IN EACH CASE HAS BEEN HIGHLIGHTED IN BOLDFACE. η IS THE SIMILARITY INDEX.

no.	η_K	$\eta_{\text{micro-DE}}$	no.	η_K	$\eta_{\text{micro-DE}}$
1	89.88	**97.85**	9	**93.47**	82.45
2	**99.44**	98.40	10	**98.32**	84.48
3	77.84	**79.85**	11	78.19	**91.18**
4	41.49	**96.14**	12	99.83	99.57
5	**92.83**	90.05	13	28.14	**99.25**
6	52.98	**57.78**	14	**97.16**	49.76
7	81.80	**93.87**	15	48.68	**97.97**
8	72.78	**99.68**	16	83.07	**98.56**

V. COMPARISON OF MICRO-DE AND MICRO-ODE

In order to accelerate micro-DE, it is equipped with opposition-based initialization (micro-ODE) [10], [19]–[24]. Because of the very small population size and also small number of required function calls to solve the objective function, the opposition-based generation jumping is not embedded in micro-ODE. Algorithm 2 presents pseudo-code for micro-ODE. The only difference between micro-DE and micro-ODE is on the population initialization. The first one uses the uniform random initialization and the second one utilizes the opposition-based initialization.

Definition (Opposite Point) - Let $P(x_1, x_2, ..., x_n)$ be a point in n-dimensional space, where $x_1, x_2, ..., x_n \in R$ and $x_i \in [a_i, b_i]$ $\forall i \in \{1, 2, ..., n\}$. The opposite point $\breve{P}(\breve{x}_1, \breve{x}_2, ..., \breve{x}_n)$ is completely defined by its components

$$\breve{x}_i = a_i + b_i - x_i. \tag{7}$$

Figure 5 illustrates a point and its corresponding opposite in one, two, and three dimensional spaces.

The minimum values for the objective function, f_{min}, for each image (kept from the micro-DE experiments), is used as value to reach (VTR) to compare convergence rate and robustness of micro-DE and micro-ODE. All control parameters are the same as before. The results

TABLE I

THRESHOLDING RESULTS. INPUT IMAGE, CORRESPONDING MANUALLY CREATED GROUND-TRUTH (GOLD) IMAGE, RESULT OF KITTLER METHOD, AND RESULT OF THE PROPOSED APPROACH (MICRO-DE).

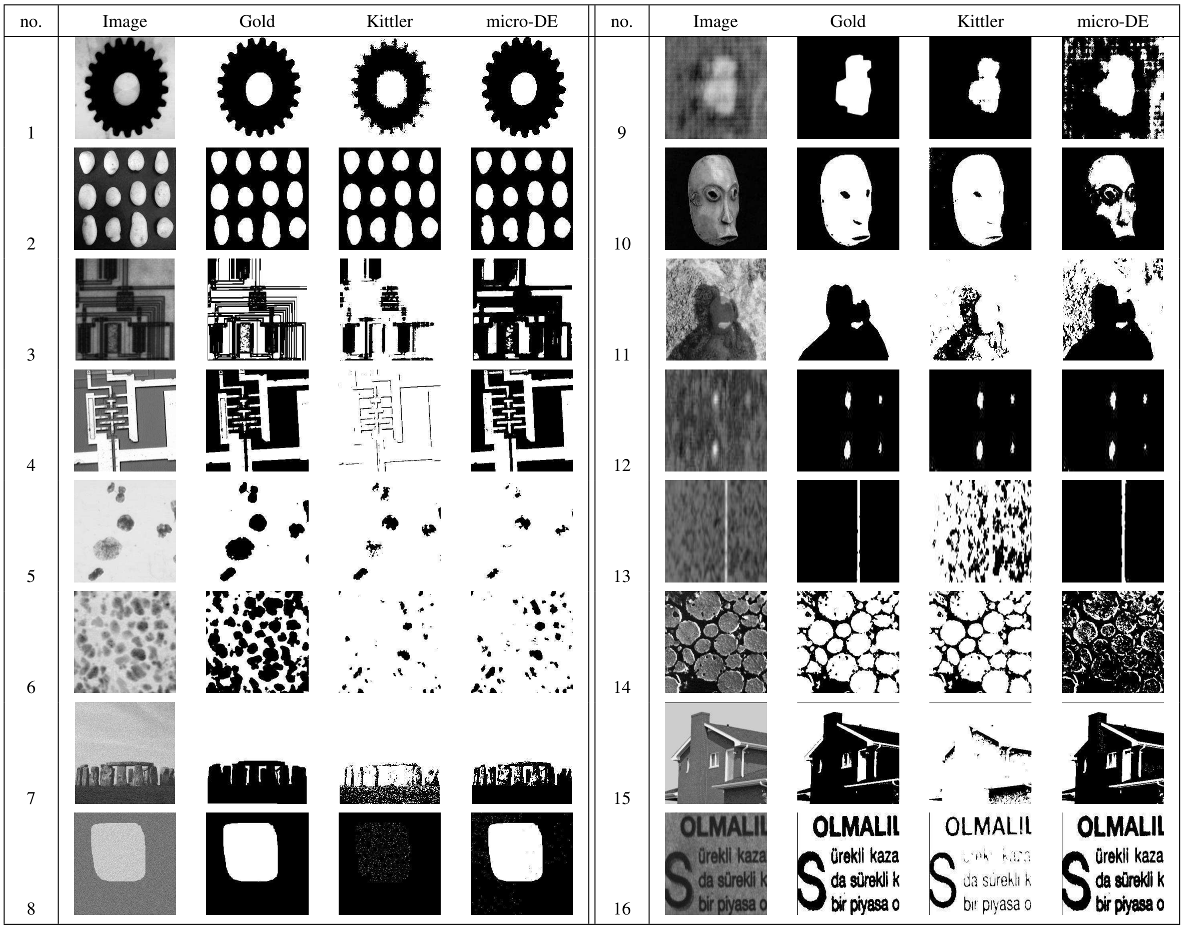

of 100 trials per image for both algorithms are summarized in Table III. Micro-ODE performs faster for 13 images. Both algorithms have the same NFCs for two images. For thresholding of 16 images, micro-DE needs 875 function calls while this number is 761 for micro-ODE (13% convergence rate improvement). The success rate (robustness) is almost the same for both (0.98 vs. 0.99). It should be mentioned, evaluation of the objective function for this optimization problem is time consuming because for each function call an image thresholding and also pixel-by-pixel comparison of two images are required. Therefore, 13% improvement at convergence rate is a valuable achievement.

VI. CONCLUDING REMARKS

In this paper, micro-DE segmented the image into two classes by minimizing the dissimilarity between input grey-level image and binary (thresholded) image. The proposed approach was compared with a well-known method, the Kittler, through an objective assessment. Results confirmed that the proposed approach is superior to the Kittler algorithm over the selected test set.

The most important part of the proposed approach is the definition of the objective function. As seen, micro-DE, as an optimizer, minimizes the dissimilarity between grey-level image and thresholded image. This dissimilarity is measured by pixel-by-pixel comparison of the binary and normalized grey-level images. The main drawback is that employing an evolutionary algorithm (DE) to threshold image shows a higher computational time. Employing the DE with a small population size (micro-DE) was in this direction to make computation time shorter. Furthermore, micro-DE was accelerated 13% by embedding opposition-based population initialization while the success rate remained the same. In

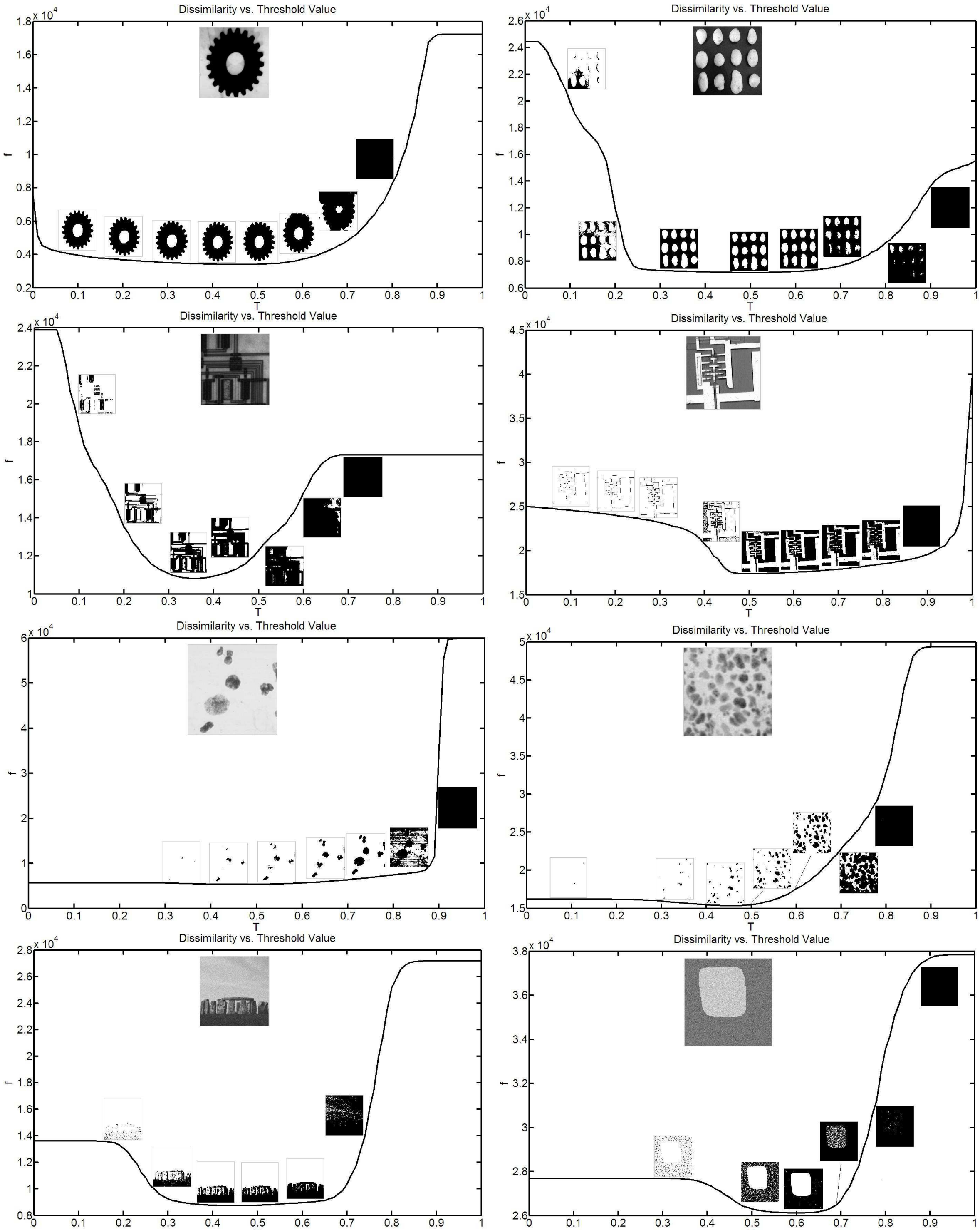

Fig. 2. Graphical illustration of dissimilarity (objective function, $f(T)$) vs. thresholding value (T). The thresholding results are presented on the curves.

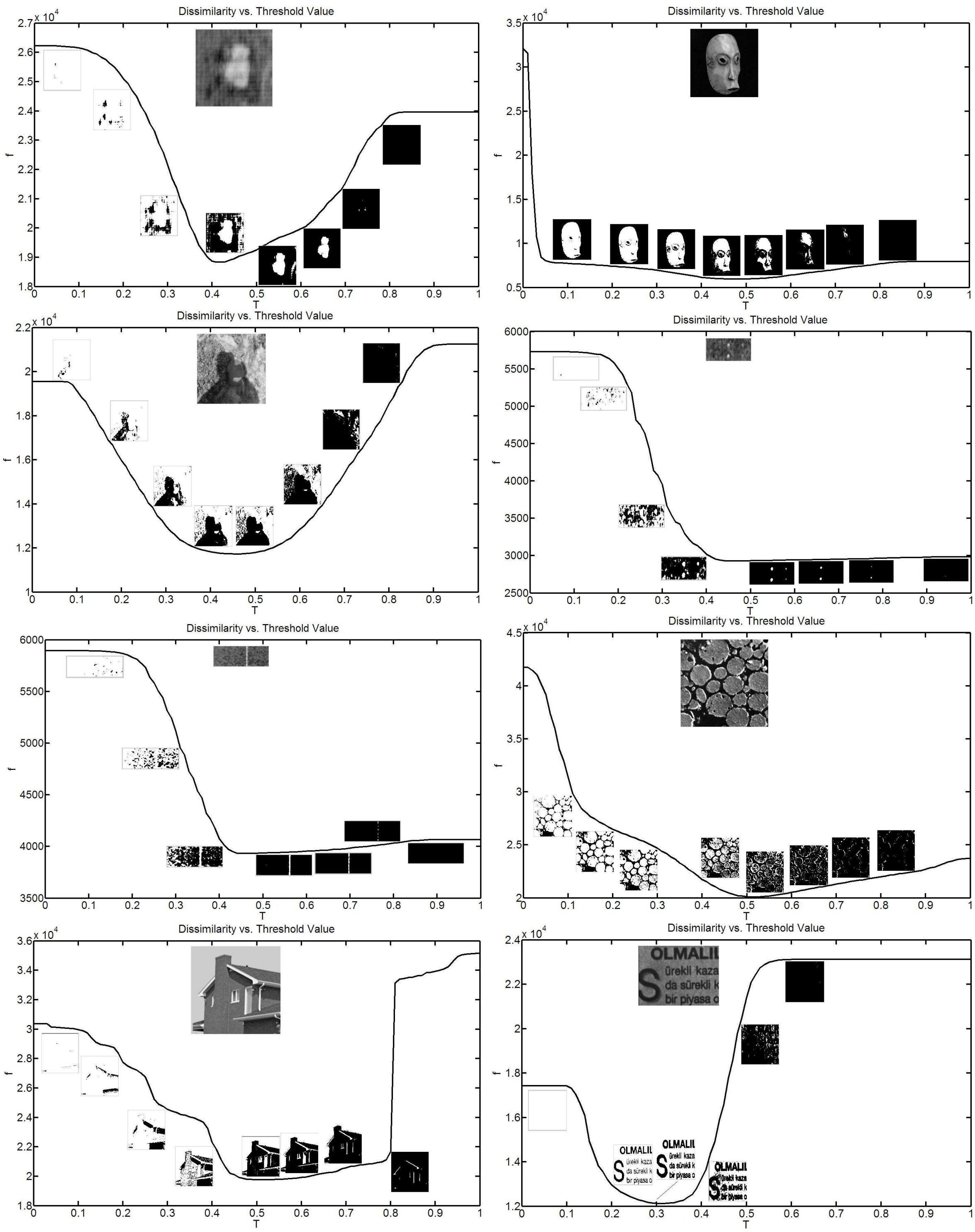

Fig. 3. Continued from Figure 2.

fact, in this paper an application of opposition-based population initialization has been introduced in image thresholding. Starting with better initial points speeds up the convergence rate of search process.

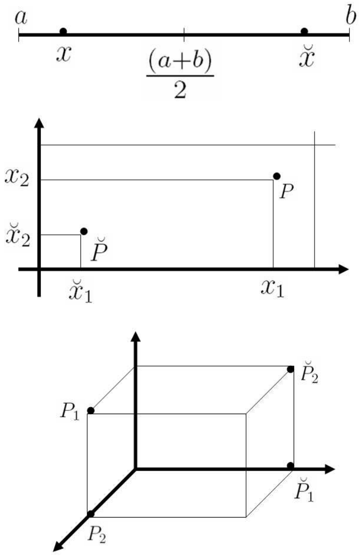

Fig. 5. Illustration of a point and its corresponding opposite in one, two, and three dimensional spaces.

TABLE III

COMPARISON OF MICRO-DE AND MICRO-ODE. REPORTED NFCS ARE THE AVERAGE OVER 100 TRIALS FOR EACH IMAGE. THE SMALLER NFC IN EACH CASE HAS BEEN INDICATED IN BOLDFACE. SR PRESENTS THE SUCCESS RATE.

		micro-DE		micro-ODE	
no.	VTR=f_{min}	*NFC*	*SR*	*NFC*	*SR*
1	3402	45	1	**36**	0.98
2	7160	44	1	**37**	1
3	10820	47	1	**34**	1
4	17385	41	0.98	**29**	1
5	5321	84	0.94	**58**	1
6	15335	77	1	**75**	0.94
7	8727	74	0.94	**64**	0.98
8	26117	58	1	**54**	1
9	18825	25	1	**21**	1
10	5944	40	1	**30**	1
11	11730	62	1	62	1
12	2929	43	1	43	1
13	3932	40	1	**36**	1
14	20088	**64**	0.98	66	0.98
15	19761	59	0.98	**50**	1
16	12123	72	1	**66**	0.98
Overall		875	0.98	**761**	**0.99**

Algorithm 2 Proposed Thresholding Approach (micro-ODE version)

Random population initialization, P_0
for $i = 0$ to N_p **do**
  for $j = 0$ to D **do**
    $OP_{0i,j} \leftarrow a_j + b_j - P_{0i,j}$
  end for
end for
Select N_p fittest individuals from set the $\{P_0, OP_0\}$ as initial population P_0
Calculate objective value (dissimilarity measure) for each individual in the population
{DE's evolution steps}
while (satisfying termination criteria) **do**
  Mutation
  Crossover
  Selection
end while
Thresholding input image with the found optimal value of thresholding level, T_{op}

The performance of the proposed image thresholding method is directly depending on the designed fitness function. As a future work direction, improving this measure by combining it with other image quality measures [25] can enhance the overall thresholding quality.

REFERENCES

[1] S. Rahnamayan, H.R. Tizhoosh, and M.M.A Salama. Automated snake initialization for the segmentation of the prostate in ultrasound images. In *Proceedings of International Conference on Image Analysis and Recognition (ICIAR-2005), Springer Lecture Notes in Computer Science Series*, pages 930–937, Toronto, Canada, Sep. 2005.

[2] N.N. Kachouie, P. Fieguth, and S. Rahnamayan. An elliptical level set method for automatic TRUS prostate image segmentation. In *Proceedings of 6th IEEE International Symposium on Signal Processing and Information Technology (ISSPIT-2006)*, pages 191–196, Vancouver, Canada, Aug. 2006.

[3] Mehmet Sezgin and Bulent Sankur. Survey over image thresholding techniques and quantative performance evaluation. *Journal of Electronic Imaging*, 13(1):146–165, 2004.

[4] H.D. Cheng, X.H. Jiang, Y. Sun, and Jingli Wang. Color image segmentation: advances and prospects. *Journal of Pattern Recognition*, 34:2259–2281, 2001.

[5] H.R. Tizhoosh. Image thresholding using type II fuzzy sets. *Journal of Pattern Recognition*, 38:2363–2372, 2005.

[6] S. Rahnamayan, H.R. Tizhoosh, and M.M.A Salama. Weighted voting-based robust image thresholding. In *Proceedings of 13th IEEE International Conference on Image Processing (ICIP-2006)*, pages 1129–1132, Atlanta, GA, USA, Oct. 2006.

[7] S. Rahnamayan, H.R. Tizhoosh, and M.M.A Salama. Image thresholding using differential evolution. In *Proceedings of the International Conference on Image Processing, Computer*

Vision, and Pattern Recognition (IPCV-2006), pages 244–249, Las Vegas, USA, June 2006.

[8] M.I. Sezan. A peak detection algorithm and its application to histogram-based image data reduction. *Journal of Computer Vision, Graphics, Image Processing*, 29:47–59, 1985.

[9] S. Rahnamayan, H.R. Tizhoosh, and M.M.A Salama. A novel population initialization method for accelerating evolutionary algorithms. *Elsvier Journal on Computers and Mathematics with Applications*, 53(10):1605–1614, 2007.

[10] S. Rahnamayan. *Opposition-Based Differential Evolution*. PhD thesis, Department of Systems Design Engineering, University of Waterloo, Waterloo, Ontario, Canada, May 2007.

[11] K. Price. *An Introduction to Differential Evolution*. McGraw-Hill, London (UK), 1999.

[12] Godfrey C. Onwubolu and B.V. Babu. *New Optimization Techniques in Engineering*. Springer, Berlin, New York, 2004.

[13] S. Das, A. Konar, and U. Chakraborty. Improved differential evolution algorithms for handling noisy optimization problems. In *Proceedings of IEEE Congress on Evolutionary Computation Conference*, pages 1691–1698, Napier University, Edinburgh, UK, September 2005.

[14] R. Storn and K. Price. Differential evolution- a simple and efficient heuristic for global optimization over continuous spaces. *Journal of Global Optimization, Kluwer*, 11:341–359, 1997.

[15] Stefan Winkler. *Vision models and quality metrics for image processing applications*. PhD thesis, École Polytechnique Fédérale de Lausanne, Switzerland, 2000.

[16] Z. Wang and A.C. Bovik. A universal image quality index. *Journal of IEEE Signal Processing Letters*, 9(3):81–84, March 2002.

[17] J.B. Martens and L. Meesters. Image dissimilarity. *Signal Processing*, 70:1164–1175, Nov. 1998.

[18] W.A. Yasnoff, J.K. Mui, and W. Bacus. Error measures for scene segmentation. *Journal of Pattern Recognition*, 9:217–231, 1977.

[19] S. Rahnamayan, H.R. Tizhoosh, and M.M.A Salama. Opposition-based differential evolution algorithms. In *Proceedings of the IEEE World Congress on Computational Intelligence (CEC-2006)*, pages 7363–7370, Vancouver, BC, Canada, July 2006.

[20] S. Rahnamayan, H.R. Tizhoosh, and M.M.A Salama. Opposition-based differential evolution for optimization of noisy problems. In *Proceedings of the IEEE World Congress on Computational Intelligence (CEC-2006)*, pages 6756–6763, Vancouver, BC, Canada, July 2006.

[21] S. Rahnamayan, H.R. Tizhoosh, and M.M.A Salama. Opposition-based differential evolution (ODE). *Journal of IEEE Transactions on Evolutionary Computation*, 12(1):64–79, Feb. 2008.

[22] S. Rahnamayan, H.R. Tizhoosh, and M.M.A Salama. Opposition versus randomness in soft computing techniques. *Elsevier Journal on Applied Soft Computing*, 8:906–918, March 2007.

[23] S. Rahnamayan, H.R. Tizhoosh, and M.M.A Salama. Opposition-based differential evolution (ODE) with variable jumping rate. In *Proceedings of IEEE Symposium on Foundations of Computational Intelligence (FOCI-2007)*, pages 81–88, Honolulu, Hawaii, USA, April 2007.

[24] S. Rahnamayan, H.R. Tizhoosh, and M.M.A Salama. Quasi-oppositional differential evolution (QODE). In *IEEE Congress on Evolutionary Computation (CEC-2007)*, pages 2229–2236, Singapore, September 2007.

[25] S. Grgić, M. Grgić, and M. Mrak. Reliability of objective picture quality measures. *Journal of Electrical Engineering*, 55(1-2):3–10, 2004.